

Effect of two different plasticizers on the properties of poly(3-hydroxybutyrate) binary and ternary blends

Irene Teresita Seoane , Liliana Beatriz Manfredi, Viviana Paola Cyras 

Instituto de Investigaciones en Ciencia y Tecnología de Materiales (INTEMA), UNMdP, CONICET, Facultad de Ingeniería, Av. Juan B Justo 4302, Mar del Plata B7608FDQ, Argentina
Correspondence to: V. P. Cyras (E-mail: vpcyras@fi.mdp.edu.ar)

ABSTRACT: Plasticized poly(3-hydroxybutyrate) (PHB) films were obtained by solvent casting. The effects of two different additives on several properties of PHB have been examined, utilizing tributyrin and poly[di(ethyleneglycol) adipate] (A). Based on changes in the glass transition temperature (T_g) and cold crystallization temperature of host PHB, the two components are miscible with PHB and they can act as plasticizers. Binary and ternary blends were obtained by adding both plasticizers separately or together, respectively. The effect of plasticizer addition on the optical transparency, water vapor permeability, and tensile properties of the films was studied. It was found that the blends remain transparent and water vapor permeability was maintained constant until a 20 wt % of plasticizer content. Plasticizing effect was corroborated and it depended on the plasticizer percentage. Binary blends had an increased plasticity, in concordance with T_g diminution of PHB. Although ternary blends presented T_g diminution, mechanical properties were not improved probably due to strong interactions between plasticizers. Finally, binary and ternary blends presented enhanced properties, causing an increment on processability. A correct knowledge between the formulation of the film and the role played by each component could allow getting custom films. © 2017 Wiley Periodicals, Inc. *J. Appl. Polym. Sci.* **2018**, *135*, 46016.

KEYWORDS: biodegradable; biopolymers and renewable polymers; thermoplastics

Received 7 June 2017; accepted 3 November 2017

DOI: 10.1002/app.46016

INTRODUCTION

Plastics are used heavily for packaging, being the fastest growing sector of the market.^{1,2} This increasing demand causes a costly impact on waste management.³ Because of this and the increasing environmental concern, biodegradable polymeric products are receiving higher attention nowadays.⁴ During the last decade, among biodegradable and biocompatible polymers, poly(3-hydroxybutyrate) (PHB) has been considered as a potential alternative for oil derived plastic materials.⁵

PHB belongs to the family of polyhydroxyalkanoates and is synthesized by a wide variety of bacteria, in general, cultivated on agricultural raw materials under stress conditions. It can be fully biodegraded to water and carbon dioxide under different environmental conditions.⁶ PHB is produced on a large scale and as thermoplastic, it can be extruded, molded, and spun using conventional processing equipment.^{7,8} Furthermore, PHB exhibits good barrier properties, transparency, water and hydrolytic resistance due to its hydrophobic character and high crystallinity.^{9,10} Because of these, this polymer is a suitable candidate for the production of biodegradable materials in different applications as films, fibers, and nonwovens, thermoformed and

injection molded rigid products, etc. However, PHB presents relative low decomposition temperature near the melting point, marked brittleness, and very low deformability which difficult its thermal processing.¹¹

In order to overcome the limitations in some properties of PHB, additives such as fillers^{12–15} or plasticizers^{16–21} can be used. Development of biodegradable materials based on PHB has become a very attractive option since PHB can be processed as a synthetic thermoplastic polymer by the addition of plasticizers. Plasticizing agents are essential generally to overcome the brittleness of the polymeric film, because reducing the intermolecular forces softens the rigidity of the film structure and increases the mobility of the polymeric chains. The primary role of a plasticizer is to improve the flexibility and processability of polymers by lowering the glass transition temperature (T_g) and it may also affect properties such as stress, hardness, density, resistance to fracture, degree of crystallinity, optical transparency, electric conductivity, and resistance to biological degradation, amongst other physical properties. In order to enhance flexibility and processability, many works introduced the use of plasticizers from available cheap materials and generally of natural origin, such as oxypropylated glycerin (or laprol),¹⁶

triacetate,¹⁷ glycerol,¹⁷ glycerol triacetate,¹⁸ acetyl tributyl citrate,¹⁹ and poly(ethylene glycol).²⁰ Yoshie *et al.*²¹ studied the degradability of PHB-based blends with natural additives, dodecanol, lauric acid, tributyrin (TB), and trilaurin. These additives (up to 9 wt %) are miscible with PHB and could retard its enzymatic degradation. Furthermore, PHB crystallinity could be reduced and its properties are improved by forming a copolymer with hydroxyvalerate monomer (PHB-HV)²² or obtaining PHB blends with an amorphous polymer²³ that could act as polymeric plasticizers, for instance poly(ethylene oxide),²⁴ poly(vinyl acetate),²⁵ poly(vinyl alcohol),²⁶ poly(L-lactic acid),²⁷ and low molar mass polyadipate.¹⁸

It is desirable that plasticizers have low mobility in the PHB matrix to avoid the migration of this additive to the surface,²¹ because that could lead to the contamination of the materials in contact with the blend causing health hazards. According to miscibility, the plasticizers with low molar mass present larger entropy for mixing than those with high molar mass.²⁸ However, monomeric plasticizers are prone to migration and consequently, plasticizers with rather high molar mass and low mobility are necessary. Polymeric plasticizers are employed as an alternative or in addition to the usual monomeric plasticizers (low molecular weight) to provide flexibility and lower modulus values in mostly poly(vinyl chloride) (PVC) blends.²⁹ Polymeric plasticizers present inherent low volatility and can also be used in combination with traditional plasticizers to reduce migration of the latter.³⁰ In addition, this type of plasticizers is able to increase thermal stability of the blend.³¹

TB, also known as glyceryl tributyrate, is naturally present in milk fat.³² It is a triglyceride used as plasticizer for cellulose esters³³ and prodrug of butyric acid with therapeutic applications.^{34,35} In general, due to the stability, low toxicity, and low vapor pressure of adipates, they are indicated to be “green” solvents. Particularly, poly[di(ethyleneglycol) adipate] (A) is a nontoxic biodegradable chemical compound used in the production of polyurethane elastomers and TPU (thermoset urethane). Also, A is a potential plasticizer of poly(L-lactic acid)^{28,36} and secondary plasticizer of PVC in ternary blends.³⁷ That is because it was selected in our work as plasticizer of PHB in order to obtain a “green” material. Currently, adipates are worldwide used as plasticizers for PVC in an extensive range of applications, but up to our knowledge it is not usually used with PHB. Using nontoxic biodegradable plasticizers, particularly macromolecules, is helpful to our health and environment. The attractive performance of A makes it a novel plasticizer for PHB in binary or ternary blends as secondary plasticizer. The

development of new techniques of plasticization is important in order to extend the applications of PHB on disposable products, compostable bags, packaging, and other specialized applications (such as biomedical implants, scaffolds, and optical films).^{38,39}

In this study, thermal, crystallization, and mechanical properties of PHB mixed with biodegradable additives were examined, in order to establish relationships between plasticizer content and film properties. The effects of different percentages of both plasticizers (TB and A) on PHB films properties were studied, comparing the response of the addition of each plasticizer separately (binary blends) and together (ternary blends). Then, a new type of ecofriendly material was analyzed, appropriate for compostable products and single use applications, such as containers and packaging, and as potential material to be processed using industrial techniques (i.e., coating paper, electrospinning, film extrusion, injection, or compression molding).

EXPERIMENTAL

Materials

PHB was kindly supplied by Biocycle, with a weight average molecular weight (M_w) of 600,000 g/mol. The product is done through the fermentation of saccharose in sugarcane by natural microorganisms of *Alcaligene* genus. *N,N*-Dimethylformamide from Cicarelli Laboratories was used as solvent. The selected additives, both from Sigma-Aldrich, were TB with molar mass of 302 g/mol and poly[di(ethyleneglycol) adipate] (A), with number average molecular weight (M_n) of 2500 g/mol.

Methods

Preparation of PHB Blends by Casting. Homogeneous solutions of PHB in *N,N*-dimethylformamide were prepared by stirring at 116 °C to ensure total dissolution. Different amounts of plasticizers, TB or A, were added to that solution in order to obtain binary blends. The samples containing 10, 20, and 30 wt % of TB plasticizer were named: PHB/10TB, PHB/20TB and PHB/30TB, respectively (idem for A). Also a combined formula of 10 wt % of each additive (ternary blend) was tested. Finally, the mix was poured into Petri dishes and kept in oven at 80 °C for 12 h to eliminate solvent by evaporation. The films were stored at room temperature for 15 days to complete PHB crystallization.

Structural and Thermal Characterization. Fourier transform infrared (FTIR) spectra were acquired with a Mattson Genesis II spectrometer, with a spectral width of 400–4000 cm^{-1} , 32 accumulations, and 4 cm^{-1} resolution. For comparison purposes, the spectra were normalized with the intensity of the band near



Figure 1. Photographs of PHB, PHB/20TB, and PHB/20A films. [Color figure can be viewed at wileyonlinelibrary.com]

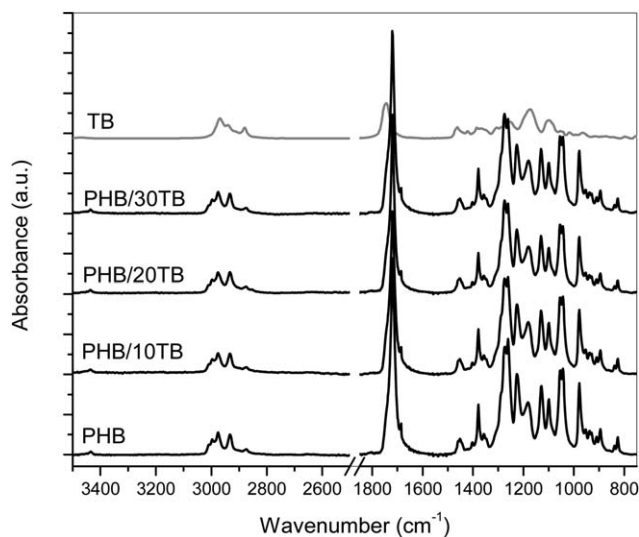


Figure 2. FTIR spectra of PHB, TB, and plasticized PHB with TB.

2933 cm^{-1} , which corresponds to the group CH_2 that is present in all samples.

Differential scanning calorimetry (DSC) analyses were carried out using a Perkin Elmer DSC instrument under nitrogen atmosphere. The first heating run was made from ambient temperature to 195 $^{\circ}\text{C}$, at a rate of 10 $^{\circ}\text{C}/\text{min}$, to determine melting temperatures (T_{m1} and T_{m2}). The temperature was maintained for 2 min to remove any prior thermal history. The samples were subsequently cooled up to -50 at 80 $^{\circ}\text{C}/\text{min}$ and kept isothermal for 2 min. Then, a second heating run was carried out at 10 $^{\circ}\text{C}/\text{min}$ from -50 to 195 $^{\circ}\text{C}$, to obtain glass transition temperature (T_g), cold crystallization temperature (T_c), and new melting temperatures. Crystallinity degree of PHB (X_{DSC}) can be determined using following equation, as a function of melting peaks area:

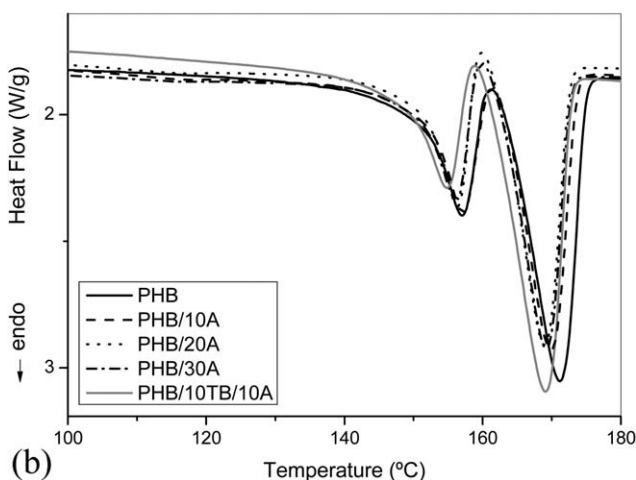
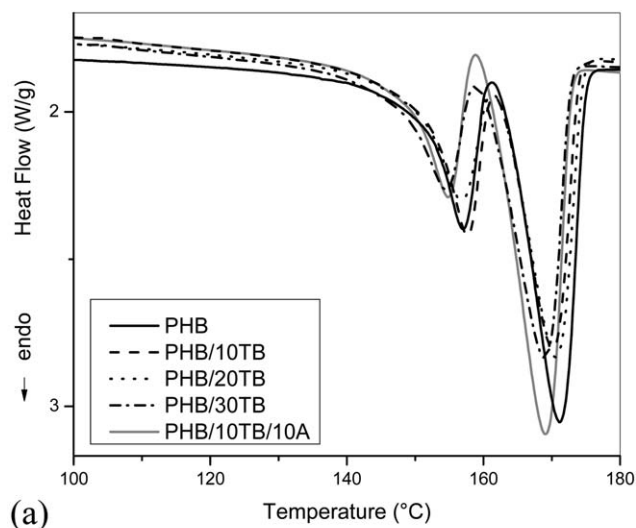


Figure 4. DSC curves of neat PHB and (a) TB and (b) A, plasticizers based samples.

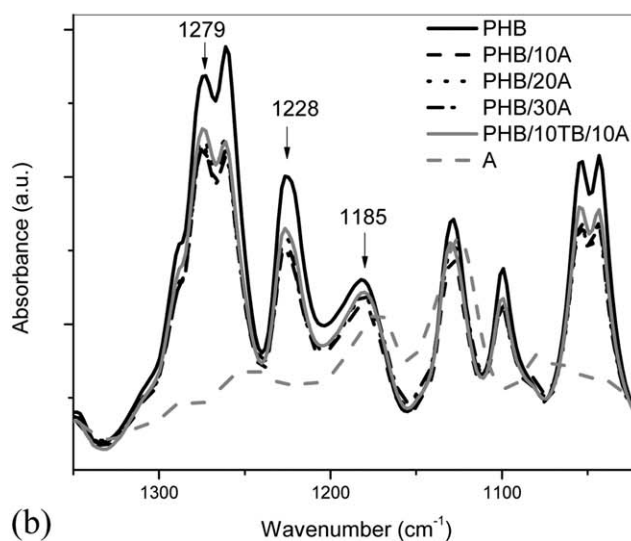
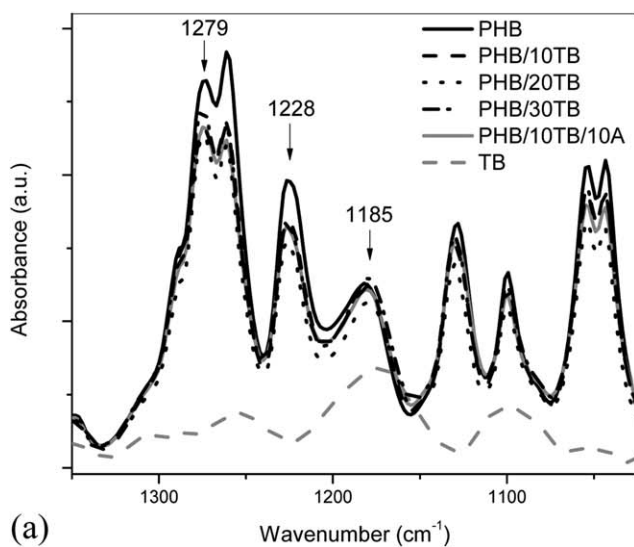


Figure 3. FTIR spectra in the 1000–1350 cm^{-1} range of PHB and plasticized PHB.

Table I. Thermal Parameters and Crystallinity of PHB and Plasticized PHB Films

Material	T_{m1} (°C) (DSC)	T_{m2} (°C) (DSC)	X_{cDSC} (%)	X_c (%) (XRD)
PHB	157.0 ± 0.5	171.0 ± 0.5	55 ± 1	66 ± 2
PHB/10TB	157.7 ± 0.1	170.1 ± 0.1	56 ± 4	63 ± 1
PHB/20TB	156.7 ± 0.4	170.7 ± 0.6	57 ± 4	66 ± 2
PHB/30TB	154.7 ± 0.1	169.0 ± 0.1	63 ± 2	64 ± 2
PHB/10A	157.3 ± 0.5	170.1 ± 0.5	53 ± 1	63 ± 2
PHB/20A	156.7 ± 0.5	169.4 ± 0.6	53 ± 2	63 ± 2
PHB/30A	156.0 ± 0.3	169.2 ± 0.2	54 ± 1	59 ± 2
PHB/10TB/10A	154.4 ± 0.5	169.0 ± 0.2	60 ± 2	59 ± 2

$$X_{cDSC} (\%) = \frac{\Delta H_m}{\Delta H_m^0 \cdot w_{PHB}} \times 100 \quad (1)$$

where ΔH_m is PHB melting enthalpy, ΔH_m^0 is the melting heat associated with pure crystalline PHB (146 J/g),⁴⁰ and w_{PHB} is the weight fraction of PHB in the blend.

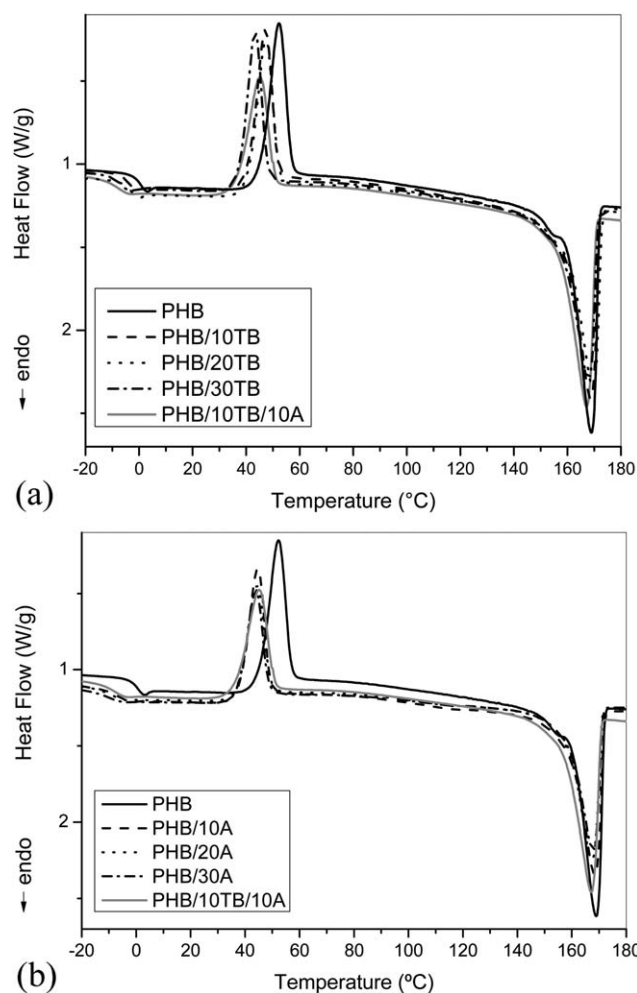
In order to determine the equilibrium melting temperature (T_m^0) of PHB and PHB blends, the samples were melted at

196 °C and quickly cooled until different isothermal crystallization temperatures (T_c^i) between 60 and 85 °C in a Perkin Elmer DSC instrument. Subsequently, samples were isothermally crystallized at fixed crystallization temperatures and then, specimens were heated to 196 °C at 10 °C/min. Finally, melting temperatures were measured. Due to the presence of two endotherms, the lowest is attributed to the melting of PHB crystals formed at the crystallization temperature and the other one is related to the material that had annealed or thickened during the heating in the DSC.⁴¹ Therefore, T_m^0 was determined by plotting the lowest experimental melting temperature of each blend (T_m^i) against corresponding T_c^i . The intersection of the experimental line with the line $T_m^i = T_c^i$ provides T_m^0 of the crystalline PHB in the corresponded blend, according to Hoffman–Weeks equation.⁴²

X-ray diffractograms were obtained with Cu-K α ($\lambda = 1.54 \text{ \AA}$) radiation in a Philips PW 1710 X-ray diffractometer system. The X-ray tube was operated at 45 kV and 30 mA, at 2°/min in the 2θ range from 5° to 60°. Crystallinity degree of the samples (X_c) could be calculated relating amorphous and crystalline areas from the diffractograms, using the equation shown below:

$$X_c (\%) = \frac{(\text{Total area}) - (\text{Amorphous area})}{(\text{Total area})} \times 100 \quad (2)$$

Thermal degradation measurements were carried out using a TA instruments Auto-MTGA Q500 Hi-Res thermogravimetric analyzer. Temperature program was run from 25 to 700 °C at a 10 °C/min heating rate under nitrogen atmosphere (30 mL/min)

**Figure 5.** DSC curves of neat PHB and (a) TB and (b) A, plasticizers based samples during second heating.**Table II.** T_g , T_c , and T_m Average Values of PHB and Plasticized PHB Films During DSC Second Heating

Material	T_g (°C)	T_c (°C)	T_m (°C)
PHB	-2.0 ± 0.2	52.7 ± 0.3	169.9 ± 0.6
PHB/10TB	-6.5 ± 0.7	46.7 ± 0.8	168.9 ± 0.2
PHB/20TB	-7.0 ± 0.9	46.6 ± 0.6	169.0 ± 0.6
PHB/30TB	-11.5 ± 0.8	45.4 ± 0.9	168.0 ± 0.7
PHB/10A	-12.2 ± 0.2	44.6 ± 0.2	168.3 ± 0.3
PHB/20A	-15.0 ± 0.6	44.5 ± 0.2	167.6 ± 0.2
PHB/30A	-16.8 ± 0.6	44.4 ± 0.2	167.7 ± 0.2
PHB/10TB/10A	-13.5 ± 0.2	45.2 ± 0.2	167.6 ± 0.5

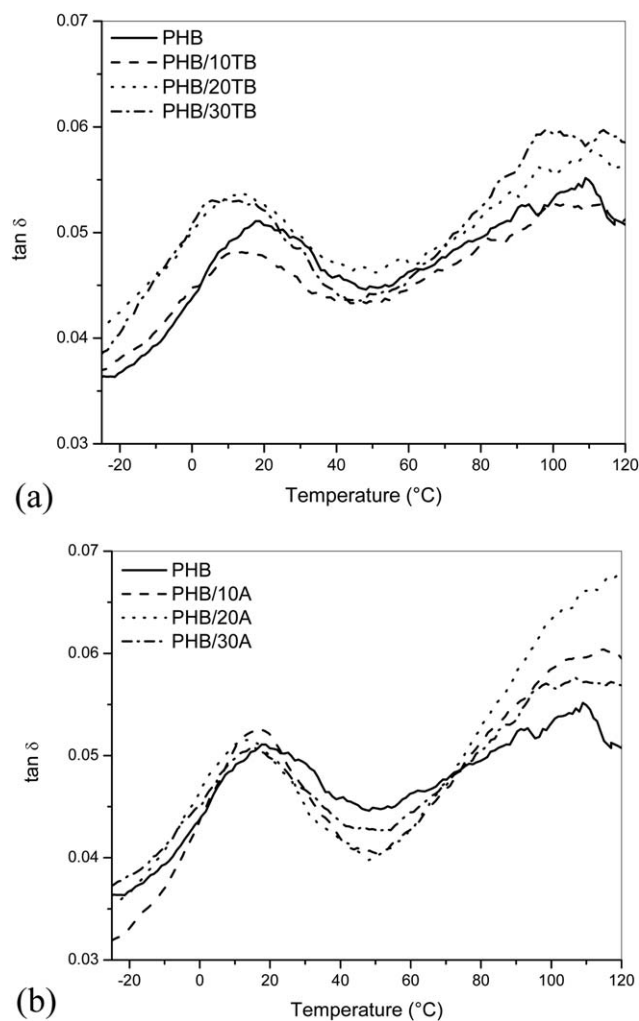


Figure 6. The $\tan \delta$ curves of neat PHB, and their blends with different amount of (a) TB and (b) A, obtained by DMA.

in order to prevent any thermo-oxidative reaction. The sample weight in all tests was approximately 10 mg.

Mechanical Characterization. Mechanical properties of the blends were determined with the INSTRON 4467 mechanical testing machine. Tensile testing of bone-shaped blend specimens was carried out using a crosshead rate of 1 mm/min (ASTM D 638–03).

Dynamic mechanical analysis was performed by means of a RHEOPLUS/32 rheometer. The frequency used was 1 Hz and the heating rate was 5 $^{\circ}\text{C}/\text{min}$, between -25 and 120 $^{\circ}\text{C}$. Each material was characterized by at least three samples.

The rheological measurements were performed at 190 $^{\circ}\text{C}$ using a rotational rheometer (MCR 301 Anton Paar) equipped with a parallel plate glass geometry (25 mm diameter). The gap between plates was 0.3 mm. Samples were equilibrated at 190 $^{\circ}\text{C}$ for 1 min before tests.

Transparency and Barrier Properties. The absorption spectra of blends, obtained in the 700–250 nm region, were investigated by Agilent 8453 UV–visible spectrophotometer.

Water vapor permeability (WVP) tests were conducted using ASTM E 96–80 method 17. Each film sample was sealed over a circular opening of 0.00177 m^2 in a permeation cell that was stored at 20 $^{\circ}\text{C}$ in desiccators. To maintain a 75% relative humidity (RH) gradient across the film, anhydrous CaCl_2 (0% RH) was placed inside the cell and a saturated NaCl solution (75% RH) was used in the desiccators. The RH inside the cell was always lower than that outside, and water vapor transport was determined from the weight gain of the permeation cell. When steady state conditions were reached (about 1 day), weight measurements were made over 10 days. Changes in the weight of the cell were recorded as a function of time with all the samples. At least three repetitions per experiment were performed.

Water vapor transmission rate is a weight gain and was calculated as the relation between the slope of each curve of weight versus time (g/s), determined by linear regression, and the cell area (m^2). Permeability was then calculated according to the following equation:

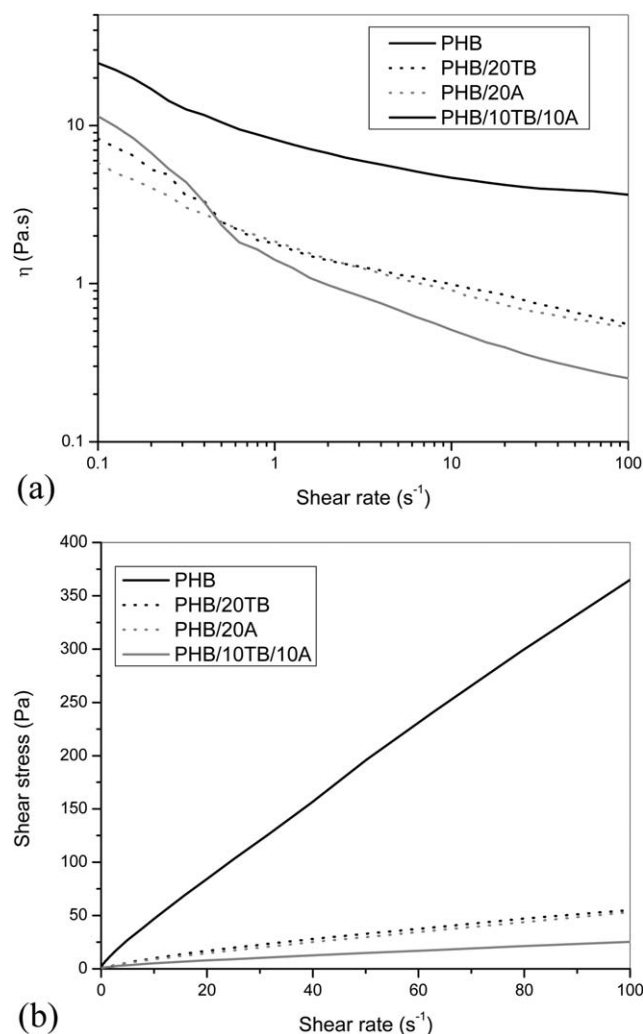


Figure 7. η (a) and shear stress (b) of PHB and PHB blends, as a function of shear rate.

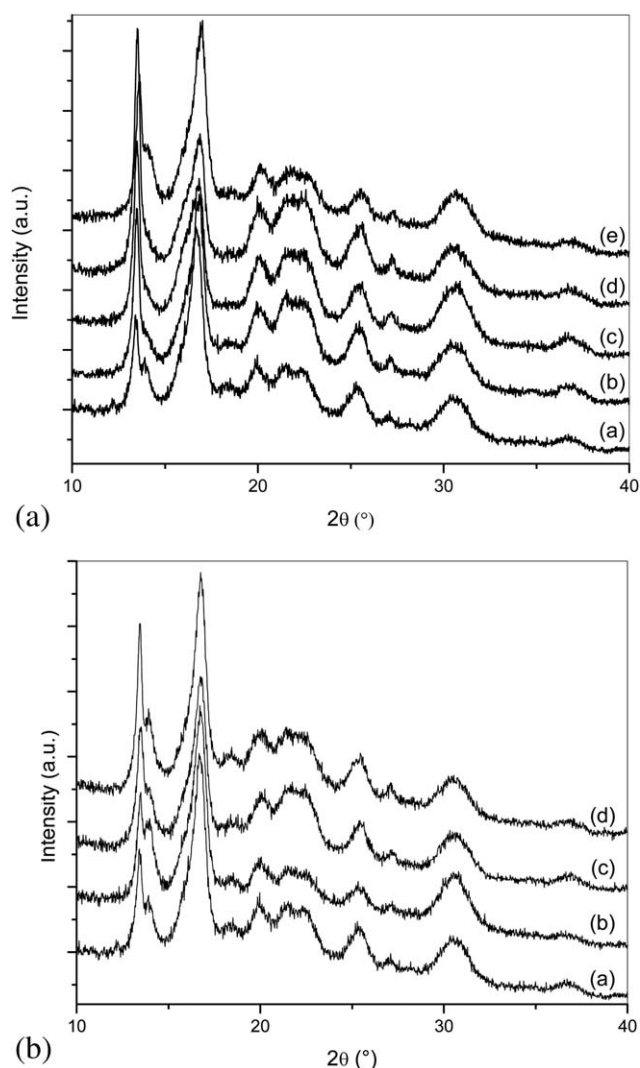


Figure 8. (a) XRD spectra of: (a) PHB, (b) PHB/10TB, (c) PHB/20TB, (d) PHB/30TB, (e) PHB/10TB/10A. (b) XRD spectra of (a) PHB, (b) PHB/10A, (c) PHB/20A, (d) PHB/30A.

$$\text{WVP} \left(\frac{g}{s \cdot m \cdot Pa} \right) = \frac{\text{WVTR}}{S \cdot (R2 - R1)} \cdot d \quad (3)$$

where S is vapor pressure of water at saturation (Pa) at test temperature (20°C), $R1$ is RH inside the permeation cell ($R1 = 0$), $R2$ is RH in the chamber ($R2 = 64.5\%$), and d is film thickness (m). Each WVP reported was the mean value of at least six samples.

RESULTS AND DISCUSSION

Structural and Thermal Properties

PHB binary and ternary blends were obtained using different percentages of TB or A as plasticizer. Figure 1 shows the photographs of PHB, PHB/20TB, and PHB/20 A films and it can be clearly seen that they are transparent.

FTIR spectra of PHB blends with TB are presented in Figure 2. Typical bands of PHB corresponding to C—O—C bond (1279, 1228, and 1185 cm^{-1}) and C=O bond (1722 and 1740 cm^{-1})

were observed. The peaks at 1279 and 1722 cm^{-1} are characteristic of the crystalline state, while the ones at 1185 and 1740 cm^{-1} correspond to the amorphous state.⁹ Similar chemical structure was observed for all the films of PHB and plasticized PHB by FTIR. In addition, the sample with both plasticizers presented a spectrum more similar to that with TB. Plasticized samples spectra presented a reduction of the intensity of PHB characteristic peaks, but crystalline peaks intensity were particularly increased with the addition of TB (Figure 3).

DSC thermograms of the neat PHB and its blends with plasticizers were obtained from the first heating at 10°C/min. The curves of TB and A plasticizers based systems are shown in Figure 4(a,b), respectively. Plasticizers effect on crystallinity and fusion temperature (T_m) was determined. Two peaks were observed in the melting region: the first one can be attributed to the melting of more irregular crystals and the second one to the most ordered crystals.⁴³ PHB crystallinity was calculated using eq. (1). It was observed that PHB crystallinity in the blends was affected by the addition of TB, increasing the heat of fusion but maintaining the value of T_m . Neither T_m nor PHB crystallinity were appreciably modified by adding A, Table I. Moreover, changes in crystallinity corroborate FTIR observations. In general, incorporation of additives into amorphous phase of a semicrystalline polymer could change its crystallinity, increasing chain mobility.²¹ Besides, the incorporation of a mix of 10% of TB and 10% of A showed a similar thermal behavior than the plasticized samples with TB or A. In addition, the obtained crystallinity by this material was intermediate between the crystallinity of samples with 20% and 30% of TB. These results indicate a synergistic plasticized effect of both additives.

Crystallization and melting behavior of the blends after thermal history erasure and a subsequent cooling run at high rate, was also studied using DSC. Second heating scans of fully amorphous samples of neat PHB, TB, and A plasticizers based formulations are shown in Figure 5(a,b), respectively. The peak corresponding to the crystallization of PHB appears during the heating process, but it occurs at less temperature for the blends than for the pristine PHB. The T_g and T_c of the samples obtained from the second heating cycle were summarized in Table II. It indicates that all PHB materials displayed a T_g between -20 and 0°C . It was observed that T_g and T_c of neat PHB were reduced in presence of plasticizers, in the binary and ternary blends. Generally, the cold crystallization occurs at a high enough temperature above the T_g of the blend, where the crystallizable polymer chains possess enough mobility to crystallize. Therefore, the reduction of blend T_g , due to a molecular motion enhancement favored by both plasticizers, could also produce T_c reduction. Besides, in the second heating scan (Figure 5), a single melting peak with a small shoulder was detected for the pristine PHB. It appears that the crystals formed during the cold crystallization are more imperfect than that formed during the casting (Figure 4), process in which crystals have more time to form. Therefore, these crystals will recrystallize and reorganize into more perfect and stable crystals during the subsequent heating scans.⁴⁴

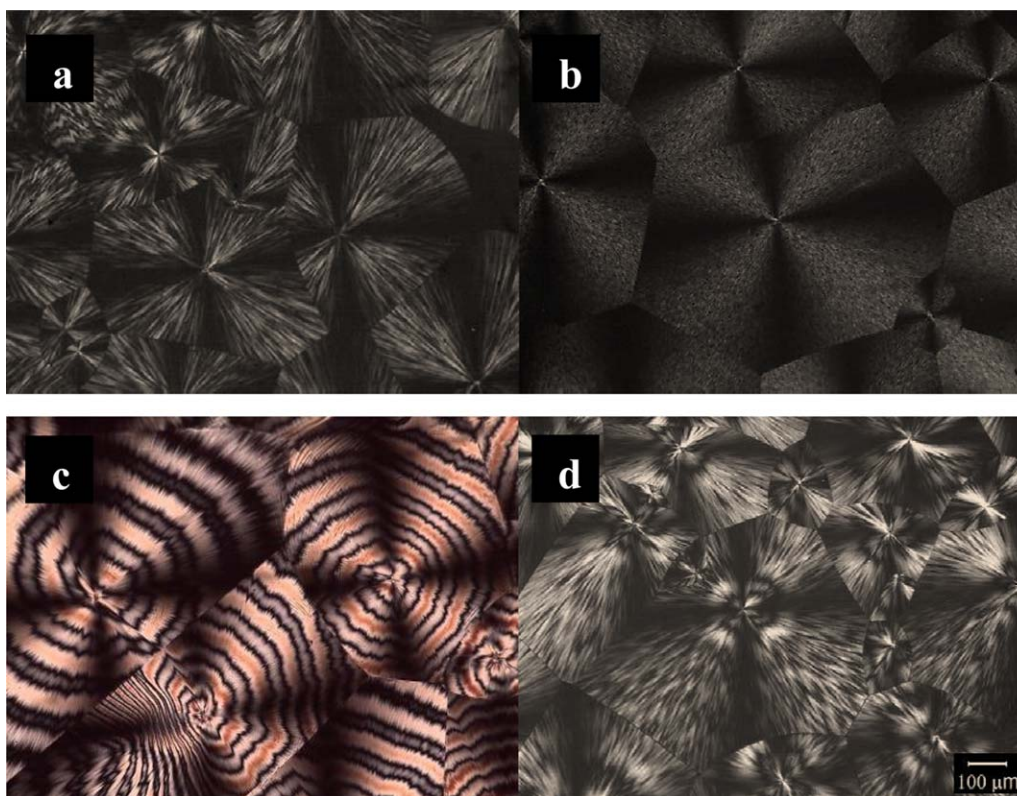


Figure 9. Spherulitic morphology of different PHB samples crystallized at 70 °C: (a) PHB, (b) PHB/20TB, (c) PHB/20A, (d) PHB/10TB/10A. [Color figure can be viewed at wileyonlinelibrary.com]

In addition, glass transition temperature of the films (T_g) was determined for all the samples by dynamic mechanical analysis, from the $\tan\delta$ curve, which is shown in Figure 6. Blends with TB showed the highest reduction in the T_g of PHB, from 18.3 (PHB) up to 9.3 (PHB/30TB). This was due to a greater increment of the polymer chains mobility by the addition of the lowest molecular weight plasticizer. While, the presence of A has little effect on the maximum $\tan\delta$ values for PHB independently of the amount, due to the high molecular weight of A. This was in accordance with the previous results.

Rheological behavior of PHB and PHB blends was investigated in order to evaluate the effect of the plasticizers on the PHB processability. The steady-state shear viscosity (η) versus shear rate curves were obtained for PHB and the samples with 20% of TB, A, or both of them, in the range from 0.01 to 100 s^{-1} of shear rates. In Figure 7, η and shear stress of the samples are presented as a function of shear rate. It was observed that shear viscosity of PHB and PHB/plasticizer blends decreased as the shear rate increased. These results indicated that PHB and the PHB blends showed shear-thinning behavior. In addition, η of PHB was reduced with the incorporation of each plasticizer separately and in combination, indicating that the studied blends formulations increase PHB processability.

Crystalline structure of the blends was studied by X-ray diffraction (XRD). In Figure 8(a,b) are presented the diffractograms of the blends with TB and A, respectively, related to PHB pattern. In Figure 6(a) is also shown the spectrum of the blend with

both plasticizers added all together. Also, samples crystallinity degree (X_c) were calculated using eq. (2) and the acquired values are listed in Table I. The calculated XRD crystallinity corresponds to global crystallinity considering that amorphous components, plasticizers, were added. It was observed that PHB crystalline structure was not modified by additives addition. Instead, the peak located at 13.4° corresponding to (0 2 0) plane of PHB crystalline pattern, improved its intensity with the

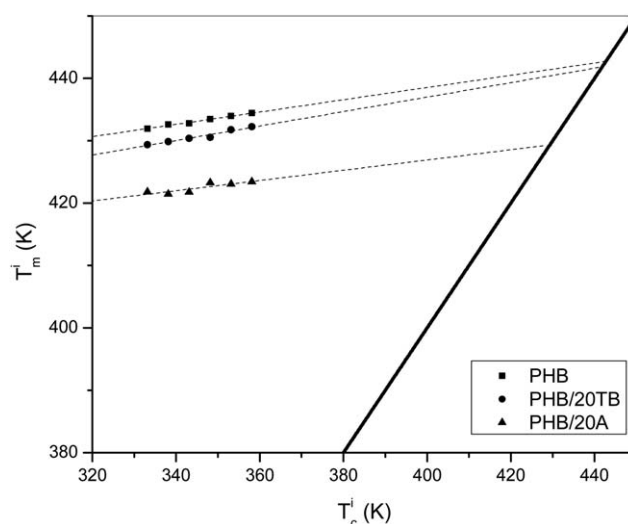


Figure 10. Plots of T_m^i versus T_c^i for PHB and different plasticized blends.

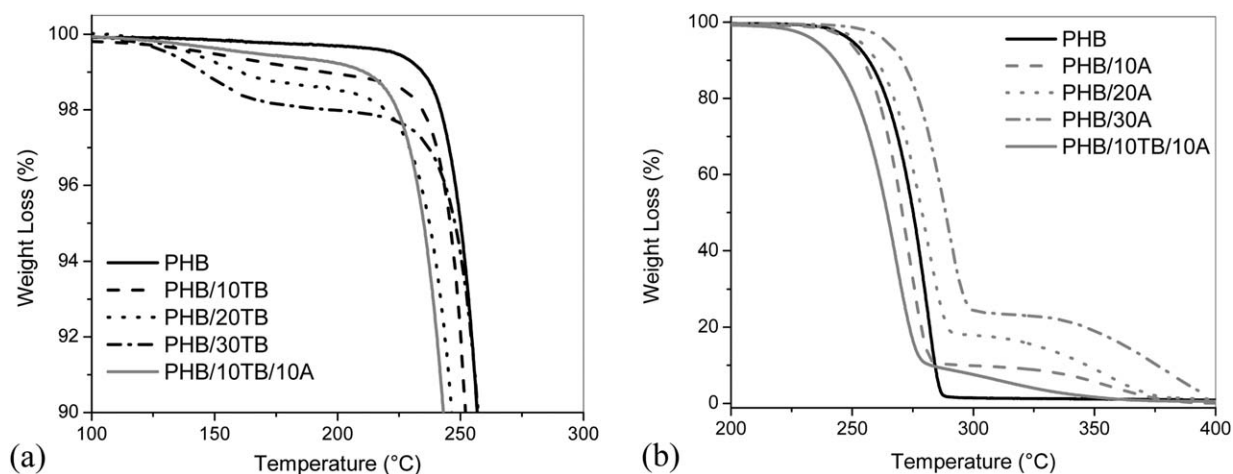


Figure 11. TGA curves of neat PHB and (a) TB and (b) A, plasticizers based samples.

addition of both additives but mainly with TB, indicating that PHB crystallinity could be enhanced. This result corroborates FTIR and DSC observations. Although matrix crystallinity in samples with TB was increased, blend crystallinity remained constant (Table I). In addition, samples with A presented a blend crystallinity reduction because of matrix crystallinity was almost maintained.

Polarized optical microscopy was used to analyze the effect of plasticizer in the spherulites morphology of binary and ternary blends. Blends samples were melted at 196 °C, quickly cooled until 70 °C, and finally maintained at this temperature. The isothermal crystallization processes were observed by optical microscopy under crossed polars, Figure 9. The observations indicated that PHB is able to crystallize according to spherulitic morphology in presence of each plasticizer. The spherulites exhibited the typical Maltese cross and no macroscopic phase separation was observed for all samples, indicating that blends are compatible in the studied composition range. Furthermore, different band spacing of the spherulites structure was observed with the addition of each plasticizer, mainly when A was added. Generally, the banded structure could be due to the existence of stress build up during crystallization that reduces the band spacing.⁴⁵ Lamellar stress could arise with the reduction of T_c^i or increase of an amorphous polymer component. Indeed, PHB spherulites exhibited band spacing reduction when crystallization temperature decreased and band pattern was extinct at T_c^i equal to 70 °C. It was identified that the addition of an amorphous polymer induces banded structure in PLA,⁴⁶ and also it could enable regular bands as it was observed in PCL blends.⁴⁷ Ma *et al.*⁴⁸ found that regularity is related with the total intermolecular interaction between the two components. Therefore, it verifies that exist an interaction between PHB and A which causes a significant modification of crystal growth processes. Moreover, PHB/A blends presented an important depression of equilibrium melting temperature (Figure 10), demonstrating miscibility between the semicrystalline polymer and the amorphous polymer.^{23,45}

Thermal stability could be affected by adding plasticizers and this was studied by thermogravimetric analysis. Weight loss versus temperature of plasticized samples with TB and A are

presented in Figure 11(a,b), respectively. The derivative thermogravimetric curves (DTG) of the blends with TB and A, related to the curves of PHB and the plasticizer, are shown in

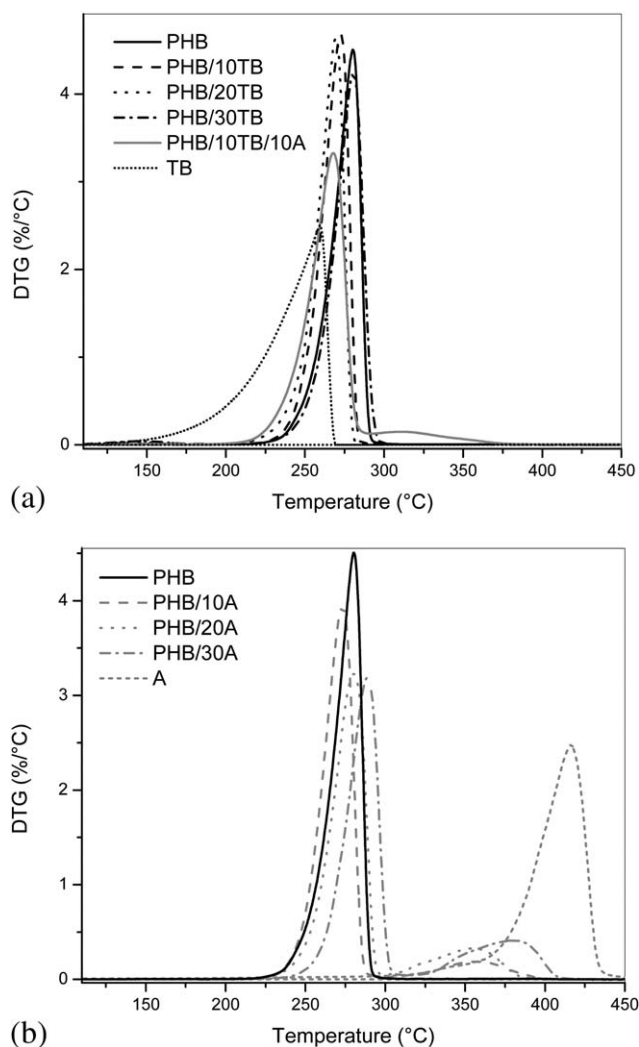


Figure 12. DTG curves of plasticized PHB samples with TB (a) and A (b) with respect to neat PHB and the corresponding plasticizer.

Table III. T_d Average Values of PHB and Plasticized PHB Films

Material	T_d (°C) (TGA)
PHB	278 ± 3
PHB/10TB	271 ± 2
PHB/20TB	272 ± 3
PHB/30TB	280 ± 3
PHB/10A	271 ± 3
PHB/20A	275 ± 3
PHB/30A	285 ± 3
PHB/10TB/10A	268 ± 2

Figure 12(a,b), respectively. The values of the degradation temperature (T_d), determined as the maximum of matrix degradation peak in DTG curves, were summarized in Table III. In the case of TB samples, degradation started at lower temperatures than PHB due to TB vaporization.^{21,49} It was clearly observed the more pronounced drop at the beginning of the weight loss curve of the plasticized samples than in that of the PHB [Figure 11(a)]. The maximum degradation temperature of PHB occurred approximately at 280 °C but this temperature was

reduced by the addition of TB [Figure 12(a)]. It could be due to the incorporation of esters groups presented in TB chemical structure, which promote catalytic degradation reactions,⁵⁰ reducing matrix T_d . However, TB addition also improved crystallization (observed by DSC) and this could recover the thermal stability of the samples by adding high percentages of plasticizer. DTG of A blends presented two peaks [Figure 12(b)], where the first was attributed to matrix degradation and second peak was related to A evaporation. It was found that the matrix thermal stability was improved with the addition of more than 20 wt % of A by increasing T_d (Table III), because the polymeric plasticizer possesses higher thermal stability than PHB.⁵¹ In the case of the ternary blend, its stability resulted more similar to blends with TB than with A, so this component could be dominant in the stability behavior. It was also observed that A evaporation temperature was reduced, as well as the loss of TB at high temperatures, these phenomena were attributed to strong interactions between plasticizers, that could be stronger than plasticizer-matrix interactions.

Mechanical Properties

Stress–strain curves of PHB and all plasticized samples are shown in Figure 13(a). The experimental results of tensile tests

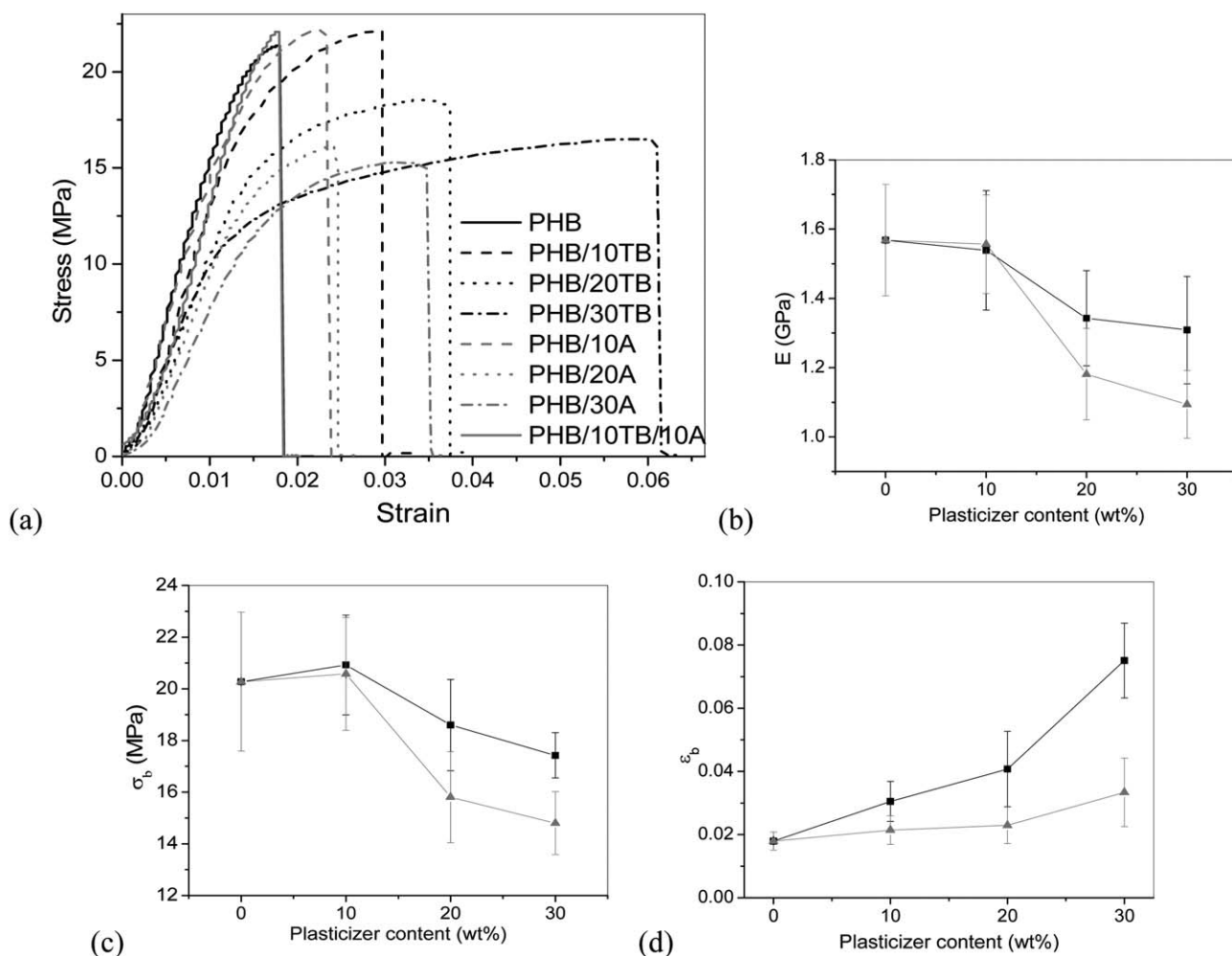


Figure 13. Stress–strain curves of PHB and plasticized PHB (a) and E (b), σ_b (c), and ϵ_b (d) as a function of TB (■) or A (▲) content.

[Young's modulus (E), tensile strength (σ_b), and elongation at break (ϵ_b)] are reported in Figure 13(b–d), respectively. The mechanical behavior of the neat PHB showed characteristics of a brittle material with a high modulus. In addition, plasticizing effect was verified through tensile tests, reducing σ_b and E , and increasing ϵ_b related to that of neat PHB.⁵² These improvements might be due to good plasticizers dispersion. Moreover, higher plasticizing effect was obtained by adding TB than A. This result indicates higher mechanical improvement by the additive with the lowest molar mass.²⁹ The addition of both plasticizers at the same time maintains the PHB mechanical properties, even though they have a combined effect in T_m , T_g , and X_c . The presence of interactions between A and TB may be the reason why mechanical properties do not improve, as it was observed by thermogravimetric analysis. In general, to achieve high ϵ_b and high degree of flexibility, the T_g must be reduced.¹⁷ However, PHB crystallinity was increased by the addition of TB and mechanical properties also depend on morphology. This latter seems to counterbalance final deformation of the PHB-based blends, restricting the application fields.

Transparency and Barrier Properties

In general, packaging prolongs content life providing protection against different factors such as light. It is desirable to obtain a translucent film with a UV (280–380 nm wavelength) and visible (380–780 nm) protection.⁵³ The optical properties of films can be affected by the addition of another component, such as plasticizers,⁵⁴ and by other factors like light wavelength, the thickness of the film, the difference between refraction indexes of the components in the mixture, porosity, and roughness.⁵⁵ UV–visible spectroscopy was carried out to determine the effect of the plasticizers (TB and A) on films transmittance (Figure 14). It was observed that transmittance was reduced similarly by both plasticizers addition. Transmittance reduction could be due to a higher light dispersion caused by the presence of a second component and the difference between refraction index of them. However, at high energy range 220–380 nm, transmittance resulted lower than 2%, indicating that plasticized films act as UV barriers. Furthermore, transmittance percentage was

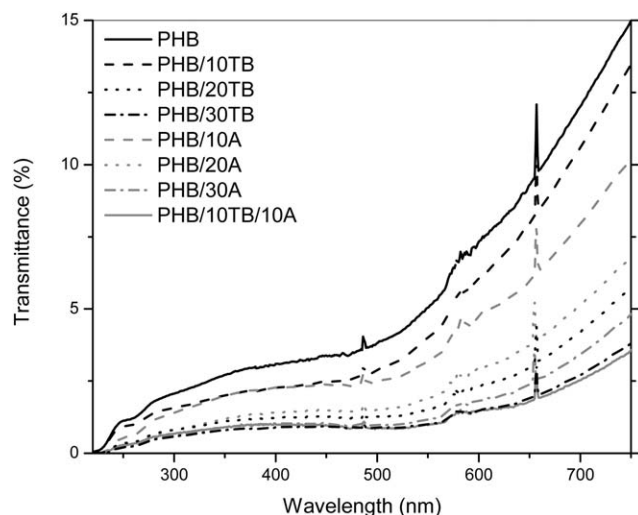


Figure 14. Transmittance curves of PHB and plasticized samples.

Table IV. WVP Values of PHB and Plasticized PHB Samples

Material	WVP $\times 10^{12}$ ($\text{g s}^{-1} \text{m}^{-1} \text{Pa}^{-1}$)
PHB	1.6 ± 0.2
PHB/10TB	1.3 ± 0.2
PHB/20TB	2.3 ± 0.3
PHB/30TB	2.6 ± 0.3
PHB/10A	1.4 ± 0.2
PHB/20A	2.3 ± 0.1
PHB/30A	2.1 ± 0.2
PHB/10TB/10A	4.1 ± 0.5

greater at visible range, in concordance with the visual observations of the films (Figure 1). The images illustrated in this figure clearly show that the transparency degree of the films was not affected by the addition of plasticizer.⁵⁶ Comparing with synthetic materials, UV barrier properties of these films were better than commodity polymers such as polypropylene, which presents 40% to 60% transmittance at the same radiation range,⁵⁷ poly(ethylene terephthalate) (PET), between 60% and 80%, and colored PET between 10% and 30%.⁵⁸

WVP tests were carried out to determine the plasticizer effect on this property of PHB. Table IV shows WVP values of native PHB and the blends with both plasticizers films. In general, plasticizer causes worsening of the water barrier properties of polymers films. The water barrier properties of plasticized films were higher beyond 20 wt % of plasticizer addition. This result could be related to free volume increment caused by addition of low molar mass additives or introduction of higher number of chain tails. Because of this, tortuosity of the water pathway is reduced, increasing diffusion through the films. In addition, there are other aspects that could influence the WVP such as the percentage of crystallinity of the PHB that slightly diminished with the content of TB and A, and then would increase the free volume.⁵⁹

CONCLUSIONS

Biodegradable transparent and homogeneous PHB plasticized films were prepared by casting with two types of plasticizers of different molar mass.

TB and A decreased the T_g of PHB in all the binary and ternary blends. The analyses of T_g and T_c in the blends showed that both additives are miscible with PHB, effectively acting as plasticizers. In addition, PHB crystallized forming a spherulitic morphology in presence of each plasticizer without macroscopic phase separation in all samples, indicating that blends are compatible in the studied composition range. Additionally, different band spacing of the spherulites structure was observed with the addition of the plasticizers, particularly when A was added.

Rheology studies shown that TB and A (in combination or separately) can decrease the shear viscosity and improve the melt fluidity of PHB.

On the other hand, thermal stability of the blends was differently affected by TB or A addition. Degradation of samples with

TB started at lower temperatures than neat PHB, due to TB vaporization. The addition of A increased PHB host stability attributed to the higher thermal stability of the polymeric plasticizer. Ternary blends presented a reduced TB loss at high temperatures, but also, matrix stability decreased. This could be ascribed to strong interactions between plasticizers.

It was observed that PHB blends show a reduction of T_g and global X_c with the addition of TB and A, which was reflected in the ϵ_b increment and σ_b reduction, whereas E was slightly reduced related to neat PHB. Although addition of both plasticizers together produced similar effect on thermal properties compared with the addition of each plasticizer separately, the mechanical properties were unaffected. Then, films morphology seems to counterbalance final deformation of the blends. At the same time, PHB exhibits good barrier properties, even though they were improved with the addition of plasticizers. Blend films presented better UV barrier properties also than commodity polymers, such as polypropylene and PET, and water permeation was maintained constant until a 20 wt % of plasticizer content. These blends seem to be suitable for single use applications, such as disposal of containers or packaging.

Another conclusion was that the polymeric plasticizer (A) caused an increment on mechanical properties in binary blends and it was also used in combination with a low molar mass plasticizer (TB), reducing the loss of the latter at high temperatures. These results would allow the development of new techniques of PHB plasticization, better management of film formulations, and an appropriate selection of plasticizer concentration in accordance with the specific requirements of potential users.

ACKNOWLEDGMENTS

The authors acknowledge the financial support of CONICET (PIP 0014 y 0527) y CNR-CONICET No. 1010, Agencia Nacional de Promoción Científica y Tecnológica (PICT'12 1983) and Universidad Nacional de Mar del Plata.

REFERENCES

1. Trinetta, V. In Reference Module in Food Science; Elsevier: Amsterdam, The Netherlands, **2016**; p 1.
2. Farmer, N. In Trends in Packaging of Food, Beverages and Other Fast-Moving Consumer Goods (FMCG); Elsevier: Amsterdam, The Netherlands, **2013**; p 288.
3. Siracusa, V.; Rocculi, P.; Romani, S.; Rosa, M. D. *Trends Food Sci. Technol.* **2008**, *19*, 634.
4. Khalil, H. P. S. A.; Davoudpour, Y.; Saurabh, C. K.; Hossain, S.; Adnan, A. S.; Dungani, R.; Paridah, M. T.; Islam Sarker, Z.; Nurul Fazita, M. R.; Syakir, M. I.; Haafiz, M. K. M. *Renew. Sustain. Energy Rev.* **2016**, *64*, 823.
5. Bugnicourt, E.; Cinelli, P.; Lazzeri, A.; Alvarez, V. *EXPRESS Polym. Lett.* **2014**, *8*, 791.
6. Bucci, D. Z.; Tavares, L. B. B.; Sell, I. *Polym. Test.* **2007**, *26*, 908.
7. Bucci, D. Z.; Tavares, L. B. B.; Sell, I. *Polym. Test.* **2005**, *24*, 564.
8. Mottin, A. C.; Ayres, E.; Eliane, A.; Oréfice, R. L.; Câmara, J. J. D. *Mater. Res.* **2016**, *19*, 57.
9. Cyras, V. P.; Galego Fernández, N.; Vázquez, A. *Polym. Int.* **1999**, *48*, 705.
10. Kumagai, Y.; Kanesawa, Y.; DOI, Y. *Makromol. Chem.* **1992**, *193*, 53.
11. de Carvalho, K. C. C.; Montoro, S. R.; Cioffi, M. O. H.; Voorwald, H. J. C. In Design and Applications of Nanostructured Polymer Blends and Nanocomposite Systems; Thomas, S., Shanks, R., Chandrasekharakurup, S., Eds.; Elsevier: Oxford, UK, **2016**; p 261.
12. Angelini, S.; Cerruti, P.; Immirzi, B.; Scarinzi, G.; Malinconico, M. *Eur. Polym. J.* **2016**, *76*, 63.
13. Reis, K. C.; Pereira, L.; Melo, I. C. N. A.; Marconcini, J. M.; Trugilho, P. F.; Tonoli, G. H. D. *Mater. Res.* **2015**, *18*, 546.
14. Seoane, I. T.; Fortunati, E.; Puglia, D.; Cyras, V. P.; Manfredi, L. B. *Polym. Int.* **2016**, *65*, 1046.
15. D'Amico, D. A.; Manfredi, L. B.; Cyras, V. P. *J. Appl. Polym. Sci.* **2012**, *123*, 200.
16. Savenkova, L.; Gercberga, Z.; Nikolaeva, V.; Dzene, A.; Bibers, I.; Kalnin, M. *Process Biochem.* **2000**, *35*, 573.
17. El-Hadi, A.; Schnabel, R.; Straube, E.; Müller, G.; Henning, S. *Polym. Test.* **2002**, *21*, 665.
18. Baltieri, R. C.; Mei, L. H. I.; Bartoli, J. *Macromol. Symp.* **2003**, *197*, 33.
19. Erceg, M.; Kovačić, T.; Klarić, I. *Polym. Degrad. Stab.* **2005**, *90*, 313.
20. Parra, D. F.; Fusaro, J.; Gaboardi, F.; Rosa, D. S. *Polym. Degrad. Stab.* **2006**, *91*, 1954.
21. Yoshie, N.; Nakasato, K.; Fujiwara, M.; Kasuya, K.; Abe, H.; DOI, Y.; Inoue, Y. *Polymer* **2000**, *41*, 3227.
22. Yoshie, N.; Fujiwara, M.; Ohmori, M.; Inoue, Y. *Polymer* **2001**, *42*, 8557.
23. Avella, M.; Martuscelli, E.; Raimo, M. *J. Mater. Sci.* **2000**, *35*, 523.
24. You, J. W.; Chiu, H. J.; Don, T. M. *Polymer* **2003**, *44*, 4355.
25. Hay, J. N.; Sharma, L. *Polymer* **2000**, *41*, 5749.
26. Azuma, Y.; Yoshie, N.; Sakurai, M.; Inoue, Y.; Chûjô, R. *Polymer* **1992**, *33*, 4763.
27. Blümm, E.; Owen, A. J. *Polymer* **1995**, *36*, 4077.
28. Okamoto, K.; Ichikawa, T.; Yokohara, T.; Yamaguchi, M. *Eur. Polym. J.* **2009**, *45*, 2304.
29. Rahman, M.; Brazel, C. S. *Prog. Polym. Sci.* **2004**, *29*, 1223.
30. Audic, J. L.; Reyx, D.; Brosse, J. C. *J. Appl. Polym. Sci.* **2003**, *89*, 1291.
31. Shah, B. L.; Shertukde, V. V. *J. Appl. Polym. Sci.* **2003**, *90*, 3278.
32. Parodi, P. W. *J. Nutr.* **1997**, *127*, 1055.
33. Encyclopedic Dictionary of Polymers; Springer: New York, NY, **2007**; p 463.
34. Chen, Z. X.; Breitman, T. R. *Cancer Res.* **1994**, *54*, 3494.

35. Ortega, J. F.; De Conti, A.; Tryndyak, V.; Furtado, K. S.; Heidor, R.; Horst, M. A.; Helena, L.; Fernandes, G.; Latorre, P. E.; Tavares, M.; Pogribna, M.; Shpileva, S.; Beland, F. A.; Pogribny, I. P.; Moreno, F. S. *Oncotarget* **2016**, *7*, 24339.
36. Liang, H.; Hao, Y.; Liu, S.; Zhang, H.; Li, Y.; Dong, L.; Zhang, H. *Polym. Bull.* **2013**, *70*, 3487.
37. Zawadzki, S. F.; Tabak, D.; Akcelrud, L. *Polym. Plast. Technol. Eng.* **1993**, *32*, 155.
38. Anbukarasu, P.; Sauvageau, D.; Elias, A. *Sci. Rep.* **2015**, *5*, 17884.
39. Wang, C.; Hsu, C.-H.; Hwang, I.-H. *Polymer* **2008**, *49*, 4188.
40. Barham, P. J.; Keller, A.; Otun, E. L.; Holmes, P. A. *J. Mater. Sci.* **1984**, *19*, 2781.
41. Organ, S. J.; Barham, P. J. *Polymer* **1993**, *34*, 2169.
42. Hoffman, J. D.; Weeks, J. J. *J. Res. Natl. Bur. Stand. Sect. A Phys. Chem.* **1962**, *66A*, 13.
43. Saeidlou, S.; Huneault, M. A.; Li, H.; Park, C. B. *Prog. Polym. Sci.* **2012**, *37*, 1657.
44. Xu, C.; Qiu, Z. *J. Polym. Sci. Part B: Polym. Phys.* **2009**, *47*, 2238.
45. Xing, P.; Dong, L.; An, Y.; Feng, Z.; Avella, M.; Martuscelli, E. *Macromolecules* **1997**, *30*, 2726.
46. Xu, J.; Guo, B.-H.; Zhou, J.-J.; Li, L.; Wu, J.; Kowalczyk, M. *Polymer* **2005**, *46*, 9176.
47. Ma, D.; Cai, H.; Zhang, J.; Luo, X. *Macromol. Chem. Phys.* **1999**, *200*, 2040.
48. Ma, D.; Zhang, J.; Wang, M.; Ma, J.; Luo, X. *Macromol. Chem. Phys.* **2001**, *202*, 961.
49. Arrieta, M. P.; Castro-López, M. d M.; Rayón, E.; Barral-Losada, L. F.; López-Vilariño, J. M.; López, J.; González-Rodríguez, M. V. *J. Agric. Food Chem.* **2014**, *62*, 10170.
50. Cyras, V. P.; Vzquez, A.; Rozsa, C.; Fernandez, N. G.; Torre, L.; Kenny, J. M. *J. Appl. Polym. Sci.* **2000**, *77*, 2889.
51. Abdelwahab, M. A.; Flynn, A.; Chiou, B. S.; Imam, S.; Orts, W.; Chiellini, E. *Polym. Degrad. Stab.* **2012**, *97*, 1822.
52. Rivero, S.; García, M. A.; Pinotti, A. *Innov. Food Sci. Emerg. Technol.* **2010**, *11*, 369.
53. Kontominas, M. G. In *Food Packaging and Shelf Life - A Practical Guide*; Robertson, G. L., Ed.; CRC Press: Boca Raton, FL, **2010**; p 81.
54. Peruzzo, P. J.; Anbinder, P. S.; Pardini, O. R.; Vega, J.; Costa, C. A.; Galembeck, F.; Amalvy, J. I. *Prog. Org. Coat.* **2011**, *72*, 429.
55. Moon, R. J.; Martini, A.; Nairn, J.; Simonsen, J.; Youngblood, J. *Chem. Soc. Rev.* **2011**, *40*, 3941.
56. Fortunati, E.; Luzi, F.; Puglia, D.; Petrucci, R.; Kenny, J. M.; Torre, L. *Ind. Crops Prod.* **2015**, *67*, 439.
57. Alin, J.; Rubino, M.; Auras, R. *J. Colloid Interface Sci.* **2015**, *456*, 155.
58. Karatapanis, A. E.; Badeka, A. V.; Riganakos, K. A.; Savvaidis, I. N.; Kontominas, M. G. *Int. Dairy J.* **2006**, *16*, 750.
59. El Miri, N.; Abdelouahdi, K.; Barakat, A.; Zahouily, M.; Fihri, A.; Solhy, A.; El Achaby, M. *Carbohydr. Polym.* **2015**, *129*, 156.